Siberian tree-ring and stable isotope proxies as indicators of temperature and moisture changes after major stratospheric volcanic eruptions

Olga V. Churakova (Sidorova)[1,2*], Marina V. Fonti[2], Matthias Saurer[3,4], Sébastien Guillet[1], Christophe Corona[5], Patrick Fonti[3], Vladimir S. Myglan[6], Alexander V. Kirdyanov[2,7,8], Oksana V. Naumova[6], Dmitriy V. Ovchinnikov[7], Alexander V. Shashkin[2,7], Irina P. Panyushkina[9], Ulf Büntgen[3,8], Malcolm K. Hughes[9], Eugene A. Vaganov[2,7,10], Rolf T.W. Siegwolf[3,4], Markus Stoffel[1,11,12]

[1]*Institute for Environmental Sciences, University of Geneva, CH-1205 Geneva, 66 Bvd Carl Vogt, Switzerland*

[2]*Institute of Ecology and Geography, Siberian Federal University RU-660049 Krasnoyarsk, Svobodniy pr 79/10, Russian Federation*

[3]*Swiss Federal Institute for Forest, Snow and Landscape Research WSL, Zürcherstrasse 111, CH-8903 Birmensdorf, Switzerland*

[4]*Paul Scherrer Institute, CH- 5232 Villigen - PSI, Switzerland*

[5]*Université Blaise Pascal, Geolab, UMR 6042 CNRS, 4 rue Ledru, F-63057 Clermont-Ferrand, France*

[6]*Institute of Humanities, Siberian Federal University RU-660049 Krasnoyarsk, Svobodniy pr 82, Russian Federation*

[7]*V.N. Sukachev Institute of Forest SB RAS, Federal Research Center "Krasnoyarsk Science Center SB RAS" RU-660036 Krasnoyarsk, Akademgorodok 50, bld. 28, Russian Federation*

[8]*Department of Geography, University of Cambridge, Downing Place, Cambridge CB2 3EN*

[9]*Laboratory of Tree-Ring Research, University of Arizona, 1215 E. Lowell St., Tucson, 85721, USA*

[10]*Siberian Federal University, Rectorate, RU-660049 Krasnoyarsk, Svobodniy pr 79/10, Russian Federation*

[11]*dendrolab.ch, Department of Earth Sciences, University of Geneva, 13 rue des Maraîchers, CH-1205 Geneva, Switzerland*

[12]*Department F.A. Forel for Environmental and Aquatic Sciences, University of Geneva, 66 Boulevard Carl-Vogt, CH-1205 Geneva, Switzerland*

Corresponding author: Olga V. Churakova (Sidorova)*

E-Mail: olga.churakova@hotmail.com

Abstract

Stratospheric volcanic eruptions have far-reaching impacts on global climate and society. Tree rings can provide valuable climatic information on these impacts across different spatial and temporal scales. To detect temperature and hydro-climatic changes after strong stratospheric Common Era (CE) volcanic eruptions for the last 1500 years (CE 535 Unknown, CE 540 Unknown, CE 1257 Samalas, CE 1640 Parker, CE 1815 Tambora, and CE 1991 Pinatubo), we measured and analyzed tree-ring width (TRW), maximum latewood density (MXD), cell wall thickness (CWT), and $\delta^{13}C$ and $\delta^{18}O$ in tree-ring cellulose chronologies of climate-sensitive larch trees from three different Siberian regions (Northeastern Yakutia - YAK, Eastern Taimyr – TAY, and Russian Altai – ALT).

All tree-ring proxies proved to encode a significant and specific climatic signal of the growing season. Our findings suggest that TRW, MXD, and CWT show strong negative summer air temperature anomalies in 536, 541-542, and 1258-1259 at all studied regions. Based on $\delta^{13}C$, 536 was extremely humid in YAK, 537-538 in TAY. No extreme hydro-climatic anomalies occurred in Siberia after the volcanic eruptions in 1640, 1815 and 1991, except for 1817 in ALT. The signal stored in $\delta^{18}O$ indicated significantly lower summer sunshine duration in 542, 1258-1259 in YAK, and 536 in ALT. Our results show that trees growing at YAK and ALT mainly responded the first year after the eruptions, whereas at TAY, the growth response occurred after two years.

The fact that differences exist in climate responses to volcanic eruptions – both in space and time – underlines the added value of a multiple tree-ring proxy assessment. As such, the various indicators used clearly help to provide a more realistic picture of the impact of volcanic eruption to past climate dynamics, which is fundamental for an improved understanding of climate dynamics, but also for the validation of global climate models.

Key words: Dendrochronology, $\delta^{13}C$ and $\delta^{18}O$ in tree-ring cellulose, tree-ring width, maximum latewood density, cell wall thickness, temperature, precipitation, sunshine duration, vapor pressure deficit

1. Introduction

Major stratospheric volcanic eruptions can modify the Earth's radiative balance and substantially cool the troposphere. This is due to the massive injection of sulphate aerosols, which reduce surface temperatures on timescales ranging from months to years (Robock, 2000). Volcanic aerosols significantly absorb terrestrial radiation and scatter incoming solar radiation, resulting in a cooling that has been estimated to about 0.5°C during the two years following the Mount Pinatubo eruption in June 1991 (Hansen et al., 1996).

Since trees – as living organisms – are impacted in their metabolism by environmental changes, their responses to these changes are recorded in the biomass, as it is found in tree-ring parameters (Schweingruber, 1996). The decoding of tree-ring archives is used to reconstruct past climates. A summer cooling of the Northern Hemisphere ranging from 0.6°C to 1.3°C has been reported after the strongest known volcanic eruptions of the past 1500 years (CE 1257 Samalas, 1815 Tambora and 1991 Pinatubo) based on temperature reconstructions using tree-ring width (TRW) and maximum latewood density (MXD) records (Briffa et al., 1998; Schneider et al., 2015; Stoffel et al., 2015; Wilson et al., 2016; Esper et al., 2017, 2018; Guillet et al., 2017; Barinov et al., 2018).

Climate simulations show significant changes in the precipitation regime after large volcanic eruptions. These include, among others, rainfall deficit in monsoon prone regions and in Southern Europe (Joseph and Zeng, 2011), and wetter than normal conditions in Northern Europe (Robock and Liu 1994; Gillet et al., 2004; Peng et al., 2009; Meronen et al., 2012; Iles et al., 2013; Wegmann et al., 2014). However, despite recent advances in the field, the impacts of stratospheric volcanic eruptions on hydro-climatic variability at regional scales remain largely unknown. Therefore, further knowledge about moisture anomalies is critically needed, especially at high-latitude sites where tree growth is mainly limited by summer temperatures.

As dust and aerosol particles of large volcanic eruptions affect primarily the radiation regime, three major drivers of plant growth (i.e. photosynthetic active radiation (PaR), temperature and vapor pressure deficit (VPD)) will be affected by volcanic activity. This reflects in low TRW as a result of reduced photosynthesis but even more so due to low temperature. As cell division is temperature dependent, its rate (tree-ring growth) will exponentially decrease with decreasing temperature below +3°C (Körner, 2015), outweighing the "low light / low-photosynthesis" effect by far.

Furthermore, over the last years some studies using mainly carbon isotopic signals ($\delta^{13}C$) in tree rings showed eco-physiological responses of trees to volcanic eruptions at the mid- (Battipaglia et al., 2007) or high- (Gennaretti et al., 2017) latitudes. By contrast, a combination of both carbon ($\delta^{13}C$) and oxygen ($\delta^{18}O$) isotopes in tree rings has been employed only rarely to trace volcanic eruptions in high-latitude or high-altitude proxy records (Churakova (Sidorova) et al., 2014).

Application of TRW, MXD, and cell wall thickness (CWT) as well as $\delta^{13}C$ and $\delta^{18}O$ in tree cellulose chronologies is a promising tool to disentangle hydro-climatic variability as well as winter and early spring temperatures at high-latitude and high-altitude sites (Kirdyanov et al., 2008; Sidorova et al., 2008, 2010, 2011; Churakova (Sidorova) et al., 2014; Castagneri et al., 2017). In that sense, recent CWT measurements allowed generating high-resolution, seasonal information of water and carbon limitations on growth during springs and summers (Panyushkina et al., 2003; Sidorova et al., 2011; Fonti et al., 2013; Bryukhanova et al., 2015). Depending on site conditions, $\delta^{13}C$ variations reflect light (stand density) (Loader et al., 2013), water availability (soil properties) and air humidity (proximity to open waters, i.e. rivers, lakes, swamps and orography) as these parameters have been recognized to modulate stomatal conductance (g_l) controlling carbon isotopic discrimination.

Depending on the study site, a decrease in the carbon isotope ratio can be expected after stratospheric volcanic eruptions due to limited photosynthetic activity and higher stomatal conductance, which in turn would be the result of decreased temperatures, VPD, and a reduction in light intensity. By contrast, volcanic eruptions have also been credited for an increase in photosynthesis as dust and aerosol particles cause an increased light scattering, compensating for the light reduction (Gu et al., 2003). A significant increase in $\delta^{13}C$ values in tree-ring cellulose should be interpreted as an indicator of drought (stomatal closure) or high photosynthesis (Farquhar et al., 1982). In the past, very little attention has been paid to the elemental and isotopic composition of tree rings for years during which they may have been subjected to the climatic influence of powerful, but remote, and often tropical, volcanic eruptions.

In this study, we aim to fill this gap by investigating the response of different components of the Siberian climate system (i.e. temperature, precipitations, VPD, and sunshine duration) to stratospheric volcanic events of the last 1500 years. By doing so, we seek to extend our understanding of the effects of volcanic eruptions on climate by combining multiple climate-sensitive variables measured in tree rings that were clustered around the time of the major volcanic eruptions (Table 1). We focus our investigation on remote tree-ring sites in Siberia, two at high latitudes (northeastern Yakutia - YAK and eastern Taimyr - TAY), and one at high altitude (Russian Altai - ALT), for which long tree-ring chronologies were developed previously with highly climate sensitive trees. We assemble a dataset from five tree-ring proxies: TRW, MXD, CWT, $\delta^{13}C$ and $\delta^{18}O$ in larch tree-ring cellulose chronologies in order to: (1) determine the major climatic drivers of the tree-ring proxies and to evaluate their individual and integrative response to climate change, and to (2) reconstruct the climatic impacts of volcanic eruptions over specific periods of the past (Table 1).

2. Material and methods

2.1. Study sites

The study sites are situated in Siberia (Russian Federation), far away from industrial centers (and 1500–3400 km apart from each other), in the zone of continuous permafrost in north-eastern Yakutia (YAK: 69°N, 148°E) and eastern Taimyr (TAY: 70°N, 103°E), and mountain permafrost in Altai (ALT: 50°N, 89°E) (Fig. 1a, Table 2). Tree-ring samples were collected during several field trips and included old relict wood and living larch trees: *Larix cajanderi* Mayr (up to 1216 years) in YAK, *Larix gmelinii* Rupr. (max. 640 years) in TAY and *Larix sibirica* Ldb. (max. 950 years) in ALT. TRW chronologies have been developed and published in the past (Fig. 1, Hughes et al., 1999; Sidorova and Naurzbaev, 2002; Sidorova, 2003 for YAK; Naurzbaev et al., 2002; Panyushkina et al., 2003 for TAY; Myglan et al., 2008 for ALT).

Due to the remote location of our study sites, we used meteorological data from monitored weather stations located at distances ranging from 50-200 km from the sampled sites. Temperature data from these weather stations are significantly correlated ($r>0.91$; $p<0.05$) with gridded data (http://climexp.knmi.nl). However, poor correlation is found with precipitation data ($r<0.45$; $p<0.05$), which most likely is the result of local topography (Churakova (Sidorova) et al., 2016).

Mean annual air temperature is lower at the high-latitude YAK and TAY sites than at the high-altitude ALT site (Table 2). Annual precipitation is low (153-269 mm yr^{-1}) at all sites. The growing season calculated with the tree growth threshold of +5ºC (Fritts, 1976; Schweingruber, 1996) is very short (50-120 days) at all locations (Table 2). Sunshine duration is higher at YAK and TAY (ca. 18-20 h/day in summer) compared to ALT (ca. 18 h/day in summer) (Sidorova et al., 2005; Myglan et al., 2008; Sidorova et al., 2011; Churakova (Sidorova) et al., 2014).

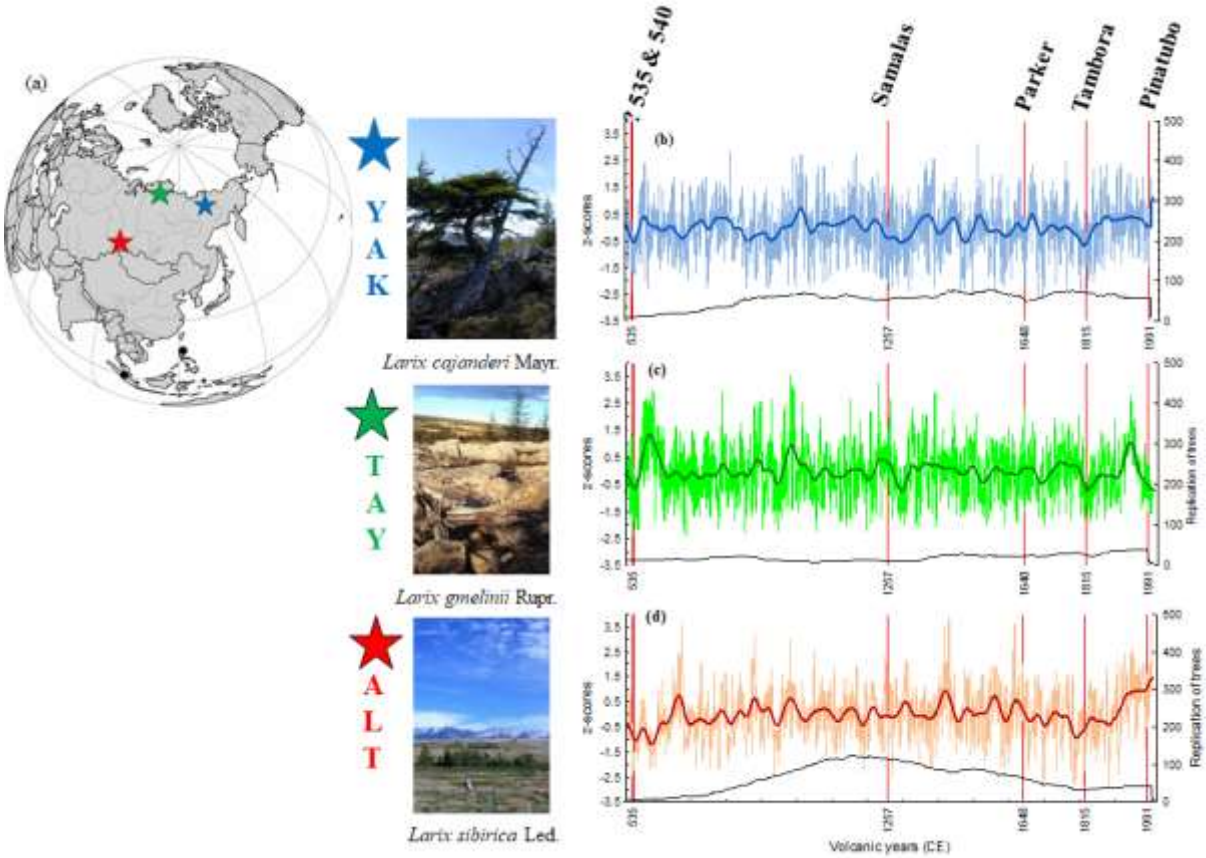

Fig. 1. Location of the study sites (stars) and known volcanos from the tropics (black dots) considered in this study (a). Annual tree-ring width index (light lines) and smoothed by 51-year Hamming window (bold lines) from the northeastern Yakutia (YAK - **blue**, b) (Hughes et al., 1999; Sidorova and Naurzbaev, 2002; Sidorova, 2003), eastern Taimyr (TAY - **green**, c) (Naurzbaev et al., 2002), and Russian Altai (ALT - **red**, d) (Myglan et al., 2009). Photos show the larch stnads at YAK, TAY (M.M. Naurzbaev) and ALT (V.S. Myglan) sites.

2.2. Selection of volcanic events and larch subsamples

Identification of the events used in this study was based on volcanic aerosols deposited in ice core records (Zielinski 1994; Robock 2000), and more precisely on Toohey and Sigl (2017), where the authors listed the top 20 eruptions over the past 2000 years, based on volcanic stratospheric sulfur injection (VSSI). From that list, we selected those reconstructed VSSI

188 and events that are well recorded in tree-ring proxies and may thus have had a noticeable im-
189 pact on the forest ecosystems in high-latitude and high-altitude regions (Briffa et al., 1998;
190 D'Arrigo et al., 2001; Churakova (Sidorova) et al., 2014; Büntgen et al., 2016; Gennaretti et
191 al., 2017; Helama et al., 2018). Therefore, based on our previously published TRW and de-
192 veloped MXD, CWT, $\delta^{13}C$ and $\delta^{18}O$ in tree-ring cellulose chronologies, we selected the peri-
193 ods CE 520-560, 1242-1286, 1625-1660, 1790-1835, and 1950-2000 with strong volcanic
194 eruptions in CE 535, 540, 1257, 1640, 1815, and 1991, as they have had far-reaching climatic
195 effects (Table 1). The recent period 1950-2000 is used to calibrate the tree-ring proxy against
196 available climate data.
197 Tree-ring material was prepared from the 2000-year TRW chronologies available at each of
198 site from the previous studies (Fig. 1 b-d). According to the level of conservation of the mate-
199 rial, the largest possible number of samples was prepared for each of the proxies. Unlike
200 TRW, which could be measured on virtually all samples, some of the material was not availa-
201 ble with sufficient quality to allow for tree-ring anatomy and stable isotope analysis. We
202 therefore use a smaller sample size for CWT (n=4) and stable isotopes (n=4) than for TRW
203 (n=12) or MXD (n=12). Nonetheless, replications are still comparable with those used in ref-
204 erence papers on stable isotopes and CWT (Loader et al., 1997; Panyushkina et al., 2003).
205
206

Table 1. List of stratospheric volcanic eruptions used in the study.

Study period (CE)	Date of eruption Month/Day/Year	Volcano name	Volcanic Explosivity Index (VEI)	Location, coordinates	References
520-560	NA/NA/535	Unknown	?	Unknown	Stothers, 1984
	NA/NA/540	Unknown	?	Unknown	Sigl et al., 2015; Toohey, Sigl 2017
1242-1286	May-October/NA/ 1257	Samalas	7	Indonesia, 8.42°N, 116.47°E	Stothers, 2000; Lavigne et al., 2013; Sigl et al., 2015
1625-1660	December/26/1640	Parker	5	Philippines, 6°N, 124°E	Zielinski et al., 1994; 2000
1790-1835	April/10/1815	Tambora	7	Indonesia, 8°S, 118°E	Zielinski et al., 1994; 2000
1950 - 2000	June/15/1991	Pinatubo	6	Philippines, 15°N, 120°E	Zielinski et al., 1994; Sigl et al., 2015

NA – not available.

Table 2. Tree-ring sites in northeastern Yakutia (YAK), eastern Taimyr (TAY), and Altai (ALT) and weather stations used in the study. Monthly air temperature (T, °C), precipitation (P, mm), sunshine duration (S, h/month) and vapor pressure deficit (VPD, kPa) data were downloaded from the meteorological database: http://aisori.meteo.ru/ClimateR.

Site	Tree species	Location	Weather station	Meteorological parameters				Length of growing season (day)	Thawing permafrost depth (max, cm)	Annual air temperature (°C)	Annual precipitation (mm)
				T (°C) Periods	P (mm)	S (h/month)	VPD (kPa)				
YAK	*Larix cajanderi* Mayr.	69°N, 148°E	Chokurdach 62°N, 147°E, 61 m. a.s.l.	1950-2000	1966-2000	1961-2000	1950-2000	50-70*	20-50*	-14.7	205
TAY	*Larix gmelinii* Rupr.	70°N, 103°E	Khatanga 71°N, 102°E, 33m. a.s.l.	1950-2000	1966-2000	1961-2000	1950-2000	90**	40-60**	-13.2	269
ALT	*Larix sibirica* Ledeb.	50°N, 89°E	Mugur Aksy 50°N, 90°E 1850 m. a.s.l.	1963-2000	1966-2000			90-120***	80-100***	-2.7	153
			Kosh-Agach 50°N, 88°E 1758 m.a.s.l.			1961-2000	1950-2000				

*Abaimov et al., 1996; Hughes et al., 1999; Churakova (Sidorova) et al., 2016

**Naurzbaev et al., 2002

***Sidorova et al., 2011

219 *2.3. Tree-ring width analysis*

220 Ring width of 12 trees was re-measured for each selected period. Cross-dating was checked by
221 comparison with the existing full-length 2000-yr TRW chronologies (Fig. 1). The TRW series
222 were standardized using the ARSTAN program (Cook and Krusic, 2008) with negative exponen-
223 tial curve (k>0) or a linear regression (any slope) prior to bi-weight robust averaging (Cook and
224 Kairiukstis, 1990). Signal strength in the regional TRW chronologies was assessed with the Ex-
225 pressed Population Signal (EPS) statistics as it measures how well the finite sample chronology
226 compares with a theoretical population chronology with an infinite number of trees (Wigley et
227 al., 1984). Mean inter-series correlation (RBAR) and EPS values of stable isotope chronologies
228 were calculated for the period 1950-2000, for which individual trees were analyzed separately.
229 All series have RBAR ranges between 0.59 and 0.87, and the common signal exceeds the EPS
230 threshold of 0.85. Before 1950, we used pooled cellulose only. For all other tree-ring parameters
231 and studied periods, the EPS exceeds the threshold of 0.85, and RBAR values range from 0.63 to
232 0.94.

233

234 *2.4. Image analysis of cell wall thickness (CWT)*

235 Analysis of wood anatomy was performed for all studied periods with an AxioVision scanner
236 (Carl Zeiss, Germany). Micro-sections were prepared using a sliding microtome and stained with
237 methyl blue (Furst, 1979). Tracheids in each tree ring were measured along five radial files of
238 cells (Munro et al., 1996; Vaganov et al., 2006) selected for their larger tangential cell diameter
239 (T). For each tracheid, CWT was computed separately. In a second step, tracheid anatomical pa-
240 rameters were averaged for each tree ring. Site chronologies are presented for the complete an-
241 nual ring chronology without standardization due to the lack of low-frequency trend. CWT data
242 from ALT for the periods 1790-1835 and 1950-2000 were used from the past studies (Sidorova
243 et al., 2011; Fonti et al., 2013) and for YAK for the period from 1600-1980 from Panyushkina et

al. (2003). Unfortunately, the remaining sample material for the CE 536 ring at TAY was insufficient to produce a clear signal. As a result, CWT is missing for CE 536 at TAY (Fig. 2).

2.5. Maximum latewood density (MXD)

Maximum latewood density chronologies from ALT were available continuously for the period CE 600-2007 from Schneider et al. (2015) and Kirdyanov A.V. (personal communication), and from YAK and TAY for the period CE 1790-2004 from Sidorova et al. (2010). For any other periods, at least six cross-sections and for CE 520-560 four sections are used. The wood is subsampled with a double-bladed saw at 1.2 mm thickness with the angle to the fiber direction. The samples were exposed to X-rays for 35-60 min (Schweingruber, 1996). MXD measurements were obtained at 0.01 mm resolution and brightness variations calibrated to g/cm^3 (Lenz et al., 1976; Eschbach et al., 1995) using a Walesch X-ray densitometer 2003. All MXD series were detrended in the ARSTAN program by calculating deviation from straight-line function (Fritts, 1976). Site MXD chronologies were developed for each volcanic period using the bi-weight robust averaging.

2.6. Stable carbon ($\delta^{13}C$) and oxygen ($\delta^{18}O$) isotopes in tree-ring cellulose

During photosynthetic CO_2 assimilation $^{13}CO_2$ is discriminated against $^{12}CO_2$, leaving the newly produced assimilates depleted in ^{13}C. The carbon isotope discrimination ($^{13}\Delta$) is partitioned in the diffusional component with a = 4.4‰ and the biochemical fractionation with b = 27‰, for C3 plants, during carboxylation via Rubisco. The $^{13}\Delta$ is directly proportional to the c_i/c_a ratio, where c_i is the leaf intercellular, and c_a the ambient CO_2 concentration. This ratio reflects the balance between stomatal conductance (g_l) and photosynthetic rate (A_N). A decrease in g_l at a given A_N results in a decrease of $^{13}\Delta$, as c_i/c_a decreases and vice versa. The same is true when A_N increases or decreases at a given g_l. Since CO_2 and H_2O gas exchange are strongly interlinked with the C-isotope fractionation $^{13}\Delta$ is controlled by the same environmental variables i.e. PaR, CO_2,

VPD and temperature (Farquhar et al., 1982, 1989; Cernusak et al., 2013). The oxygen isotopic compositions of tree-ring cellulose record the $\delta^{18}O$ of the source water derived from precipitation, which itself is related to temperature variations at middle and high latitudes (Craig, 1961; Dansgaard, 1964). It is modulated by evaporation at the soil surface and to a larger degree by evaporative and diffusion processes in leaves; the process is largely controlled by the vapor pressure deficit (Dongmann et al., 1972, Farquhar and Loyd, 1993, Cernusak et al., 2016). A further step of fractionation occurs as sugar molecules are transferred to the locations of growth (Roden et al., 2000). During the formation of organic compounds the biosynthetic fractionation leads to a positive shift of the $\delta^{18}O$ values by 27‰ relative to the leaf water (Sternberg, 2009). The oxygen isotope variation in tree-ring cellulose therefore reflects a mixed climate information, often dominated by a temperature, source water or sunshine duration modulated by the VPD influence. The cross-sections of relict wood and cores from living trees used for the TRW, MXD and CWT measurements were then selected for the isotope analyses. We analyzed four subsamples for each studied period according to the standards and criteria described in Loader et al. (2013). The first 50 yrs. of each sample were excluded to limit juvenile effects (McCarroll and Loader, 2004). After splitting annual rings with a scalpel, the whole wood samples were enclosed in filter bags. α-cellulose extraction was performed according to the method described by Boettger et al. (2007). For the analyses of $^{13}C/^{12}C$ and $^{18}O/^{16}O$ isotope ratios, 0.2-0.3 mg and 0.5-0.6 mg of cellulose were weighed for each annual ring, into tin and silver capsules, respectively. Carbon and oxygen isotopic ratios in cellulose were determined with an isotope ratio mass spectrometer (Delta-S, Finnigan MAT, Bremen, Germany) linked to two elemental analyzers (EA-1108, and EA-1110 Carlo Erba, Italy) via a variable open split interface (CONFLO-II, Finnigan MAT, Bremen, Germany). The $^{13}C/^{12}C$ ratio was determined separately by combustion under oxygen excess at a reactor temperature of 1020°C. Samples for $^{18}O/^{16}O$ ratio measurements were pyrolyzed to CO at 1080°C (Saurer et al., 1998). The instrument was operated in the continuous flow mode

295 for both, the C and O isotopes. The isotopic values were expressed in the delta notation multi-
296 plied by 1000 relative to the international standards (Eq. 1):

297 $$\delta \text{ sample} = R_{sample}/R_{standard}-1 \qquad \text{(Eq. 1)}$$

298 where R_{sample} is the molar fraction of $^{13}C/^{12}C$ or $^{18}O/^{16}O$ ratio of the sample and $R_{standard}$ the molar
299 fraction of the standards, Vienna Pee Dee Belemnite (VPDB) for carbon and Vienna Standard
300 Mean Ocean Water (VSMOW) for oxygen. The precision is $\sigma \pm 0.1‰$ for carbon and $\sigma \pm 0.2‰$
301 for oxygen. To remove the atmospheric $\delta^{13}C$ trend after CE 1800 from the carbon isotope values
302 in tree rings (i.e. Suess effect, due to fossil fuel combustion) we used atmospheric $\delta^{13}C$ data from
303 Francey et al. (1999), http://www.cmdl.noaa.gov./info/ftpdata.html). These corrected series were
304 used for all statistical analyses. The $\delta^{18}O$ cellulose series were not detrended.
305
306 *2.7. Climatic data*
307 Meteorological series were obtained from local weather stations close to the study sites and used
308 for the computation of correlation functions between tree-ring proxies and monthly climatic pa-
309 rameters (Table 2, http://aisori.meteo.ru/ClimateR).
310
311 *2.8. Statistical analysis*
312 All chronologies for each period were normalized to z-scores (Fig. 2). To assess post-volcanic
313 climate variability, we used Superposed Epoch Analysis (SEA, Panofsky and Brier, 1958) with
314 the five proxy chronologies available at each of the three study sites. In this study, intervals of 15
315 years before and 20 years after a volcanic eruption were analyzed. SEA is applied to the six an-
316 nually dated volcanic eruptions (Table 1).
317 To test the sensitivity of the studied tree-ring parameters to climate bootstrap correlation func-
318 tions were computed between proxy chronologies and monthly climate predictors using the
319 'bootRes' package of R software (R Core Team 2016) for the period 1950 (1966)-2000.

To estimate whether volcanic years can be considered as extreme and how anomalous they are compared to non-volcanic years, we computed Probability Density Functions (PDFs, Stirzaker, 2003) for each study site and for each tree-ring parameter over a period of 219 years for which measurements are available (Fig. S1). A year is considered (very) extreme if the value of a given parameter is below the (5^{th}) 10^{th} percentile of the PDF.

3. Results

3.1. Anomalies in tree-ring proxy chronologies after stratospheric volcanic eruptions

Normalized TRW chronologies show negative deviations the year following the eruptions at all studied sites (Fig. 2). Regarding CWT, a strong decrease is observed in CE 537 at all study sites. Only two layers of cells were formed in CE 537 (-1.8σ) and 541 (-2.4σ) for YAK as compared to the 11-20 layers of cells formed on average during "normal" years. In addition, we also observe the formation of frost rings in ALT between CE 536 and 538, as well as in 1259. An abrupt CWT decrease is recorded in TAY in 537 (-3.1σ).

Furthermore, we found decreasing MXD values at ALT (-4.4 σ) in CE 537 and YAK (-2.8 σ) in CE 536. However, for TAY, data show a less pronounced pattern of MXD variation (Fig. 2). In this regard, the sharpest decrease was observed in the CWT chronologies from YAK in CE 540 (-1.9σ) and 541 (-2.4σ), whereas the response was smaller in TAY and ALT for the same years (Fig. 2). The ALT $\delta^{18}O$ chronology recorded a drastic decrease in 536 CE with - 4.8 σ (Fig. 2, Fig. S1). A $\delta^{18}O$ decrease for YAK was found after the CE 1257 Samalas eruption in CE 1258 (-1.5 σ) and in 1259 (-2.9σ), which is opposite to the increased $\delta^{18}O$ value found in CE 1259 at ALT (Fig. 2; Fig. S1).

Regarding the carbon isotope ratio, negative anomalies are observed in ALT already in 1258 (-2.3σ). The CE 540 eruption was less clearly recorded in tree-ring proxies from TAY, compared to YAK and ALT (Fig. 2). With respect to the CE 1257 Samalas eruption (Fig. 2), the year following the eruption was recorded as very extreme in the TRW, MXD, $\delta^{18}O$, while less extreme

346 in CWT and $\delta^{13}C$ from YAK. ALT chronologies show a synchronous decrease for all proxies

347 following two years after the eruption (Fig. 2, Fig. S1).

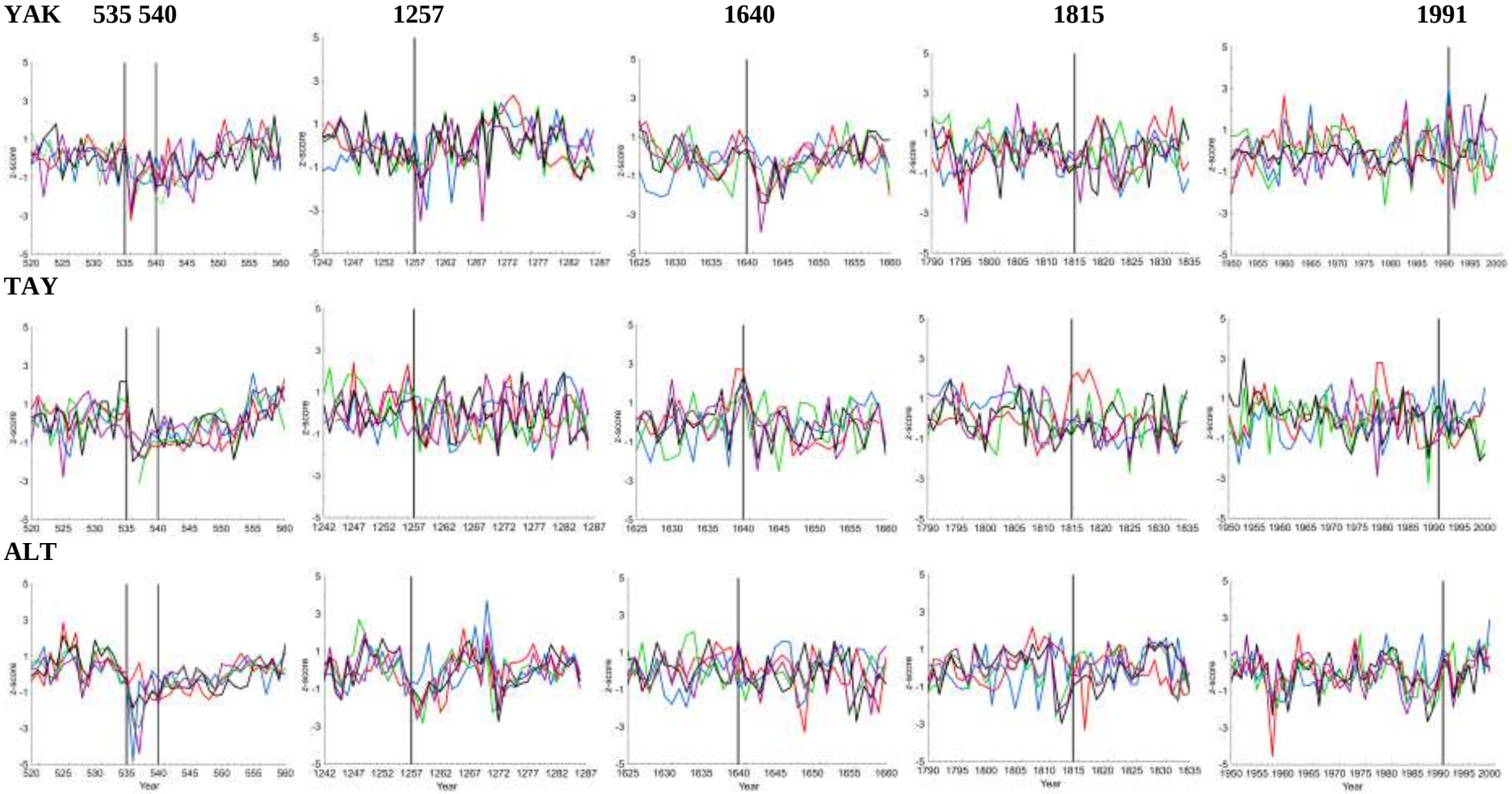

Fig. 2. Normalized (z-score) individual tree-ring index chronologies (TRW, **black**), maximum latewood density (MXD, **purple**), cell wall thickness (CWT, **green**), $\delta^{13}C$ (**red**) and $\delta^{18}O$ (**blue**) in tree-ring cellulose chronologies from northeastern Yakutia (YAK), eastern Taimyr (TAY) and Altai (ALT) for the specific periods CE 520-560, 1242-1286, 1625-1660, 1790-1835, 1950-2000 before and after the eruptions CE 535, 540, 1257, 1640, 1815 and 1991 are presented. Vertical lines show year of the eruptions.

The impacts of the more recent CE 1640 Parker, 1815 Tambora, and 1991 Pinatubo eruptions are, by contrast, far less obvious. In CE 1642, decreasing values are observed in all tree-ring proxies from the high-latitude sites YAK and TAY, whereas tree-ring proxies are not clearly affected at ALT (Fig. 2; Fig. S1).

Hardly any strong anomalies are observed in CE 1816 in Siberia regardless of the site and the tree-ring parameter analyzed. The ALT $\delta^{13}C$ value (-3.3σ) in CE 1817 and YAK MXD (-2.4σ) in 1816 can be seen as an exception to the rule here as they evidenced extreme values, respectively (Fig. S1).

Finally, the Pinatubo eruption is mainly captured by the MXD (-2.8σ) and CWT (-2.2σ) chronologies from YAK in CE 1992. Simultaneous decreases of all tree-ring proxies from ALT are observed in 1993 (Fig. 2), which, however, cannot be classified as extreme (Fig. S1).

Overall, the SEA (Fig. 3) shows that volcanic eruptions centered around CE 535, 540, 1257, 1640, 1815, and 1991 have led to decreasing values for all tree-ring proxies following next two years afterwards. A short-term response by two years after the eruptions is observed in the TRW and CWT proxies for TAY, while for YAK and ALT, the CWT decrease lasts longer (up to 5-6 years in ALT and YAK, respectively) (Fig. 3). The $\delta^{18}O$ isotope chronologies (z-score) show a distinct decrease the year after the eruptions. At ALT, however, the duration of negative anomalies were shorter (5 years) than at the high-latitude TAY (12 years) and YAK (9 years) sites. At the YAK site, two negative years followed the events, intermitted with one positive value, to remain negative during the following 7 years. The duration of negative anomalies recorded in $\delta^{13}C$ values (z-score) lasts also longer at the high-latitude YAK site - 10 years after the eruptions and 13 years at TAY compared to 7 years at ALT (Fig. 3). The largest decrease in MXD values (in terms of z-score) is found at the high-latitude YAK site. The SEA for TRW, MXD, $\delta^{13}C$, and CWT from YAK as well as TRW and MXD from

ALT show a more drastic decrease of values during the first year when compared to other proxies and study sites (Fig. 3).

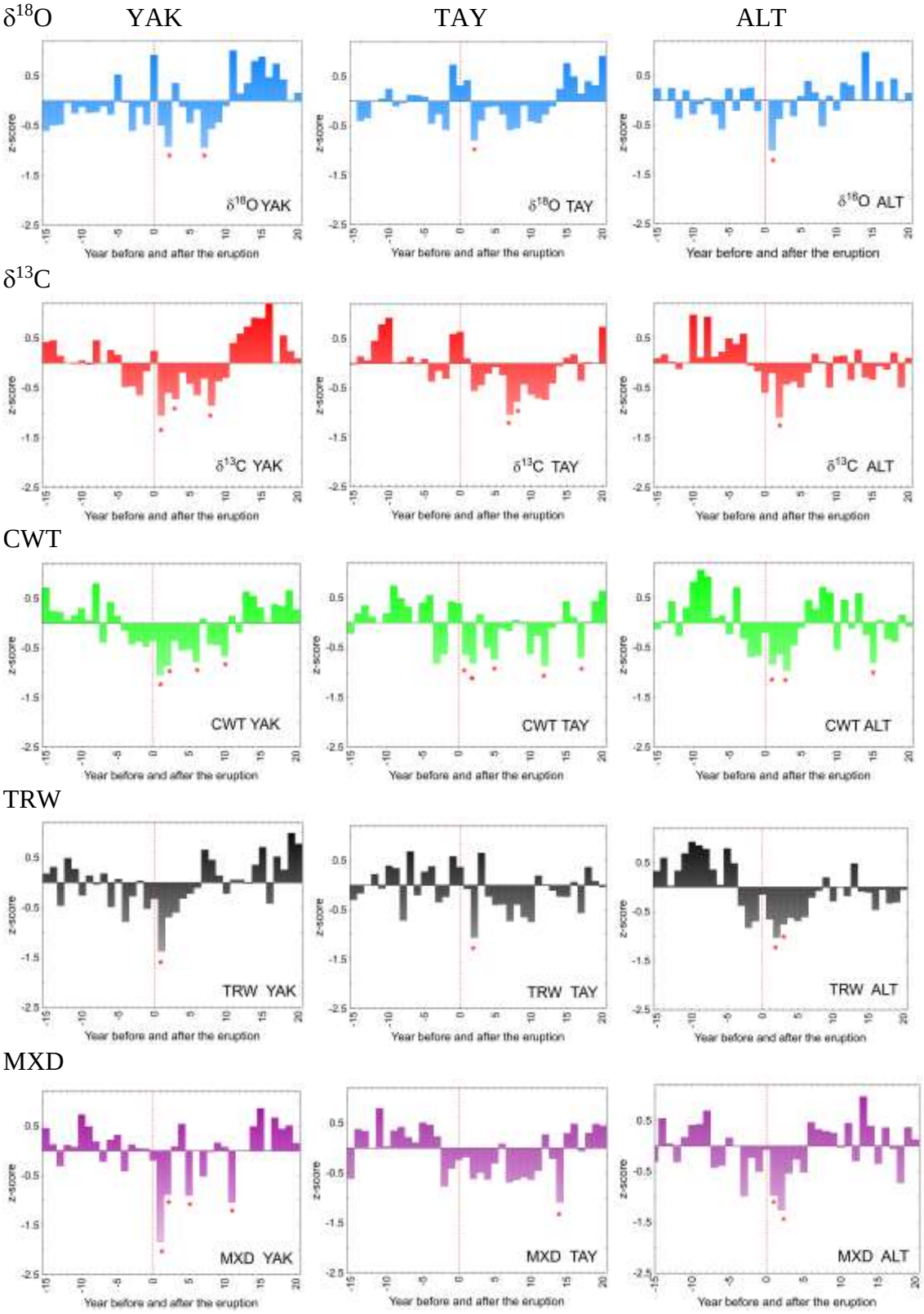

394 **Fig. 3.** Superposed epoch analysis (SEA) of $\delta^{18}O$, $\delta^{13}C$, CWT, TRW, and MXD chronologies
395 for the Yakutia (YAK), Taimyr (TAY), and Altai (ALT) sites, summarizing negative anoma-
396 lies 15 years before and 20 years after the volcanic eruptions in CE 535, 540, 1257, 1640,
397 1815, and 1991. Statistically negative anomalies are marked with a red star (*$p<0.05$).
398
399 **3.2. Tree-ring proxies versus meteorological series**
400 *3.2.1. Monthly air temperatures and sunshine duration*
401 Bootstrapped functions calculated for the instrumental period (1950-2000) show significant
402 positive correlations ($p<0.05$) between TRW and MXD chronologies and mean summer
403 (June-July) temperatures at all sites. Temperatures at the beginning (June) and the end of the
404 growing season (mid-August) influenced the MXD chronology in ALT (r = 0.57) and YAK (r
405 = 0.55), respectively (Fig. 4). July temperatures appear as a key factor for determining tree
406 growth as they significantly impact CWT, $\delta^{13}C$, and $\delta^{18}O$ (with the exception of TAY for the
407 latter) chronologies (r=0.28-0.60) at YAK and ALT.
408 Correlation analysis between July temperature and July sunshine duration indicate significant
409 ($p<0.05$) correlation for YAK (r=0.56) and ALT (r=0.34). July sunshine duration are strongly
410 and positively correlated with $\delta^{18}O$ in larch tree-ring cellulose chronologies from YAK
411 (r=0.73) and ALT (r=0.51) for the period 1961-2000 (available sunshine duration data set).

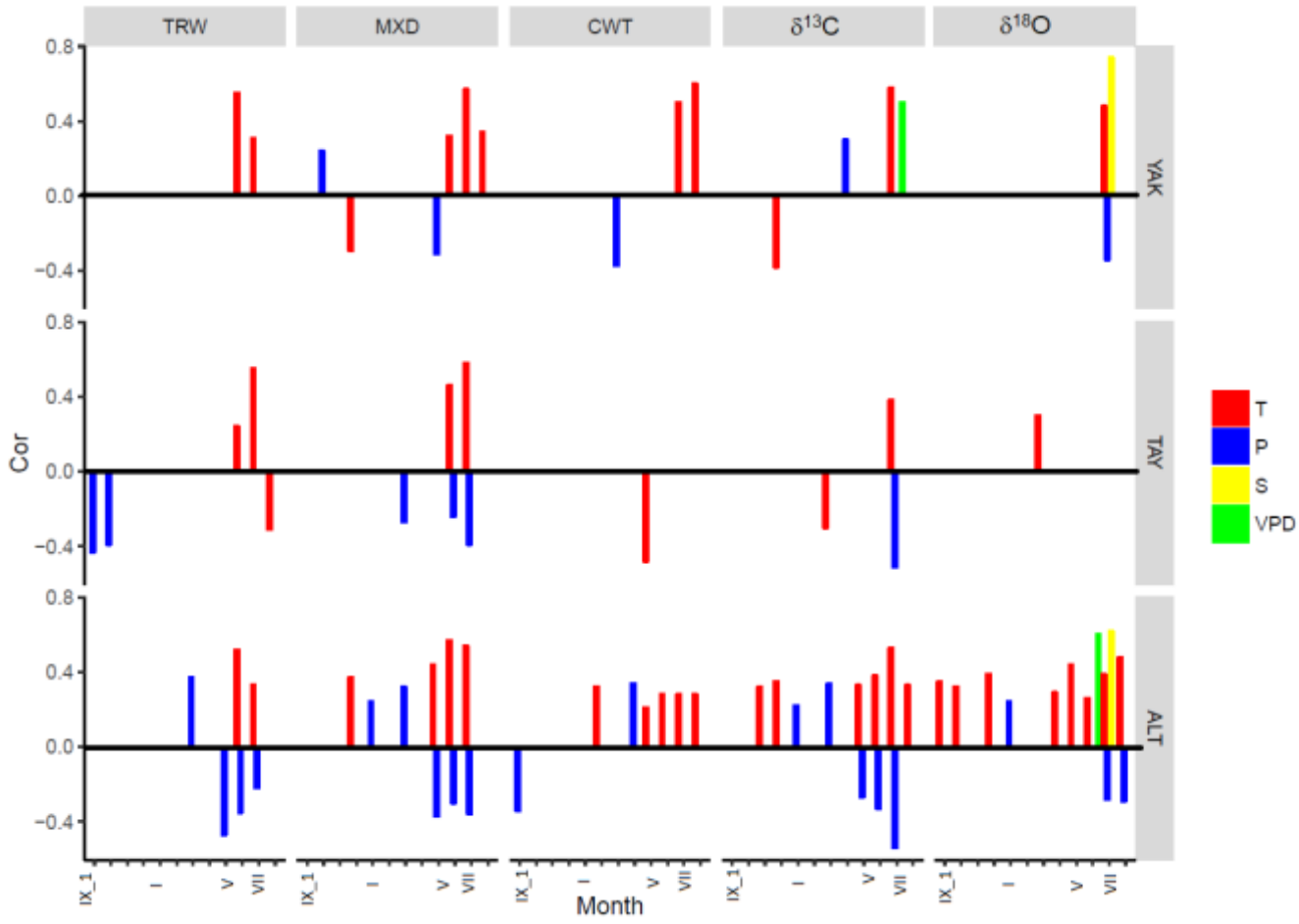

Fig. 4. Significant correlation coefficients between tree-ring parameters: TRW, MXD, CWT, $\delta^{13}C$ and $\delta^{18}O$ versus weather station data: temperature (T, red), precipitation (P, blue), vapor pressure deficit (VPD, green), and sunshine duration (S, yellow) from September of the previous year to August of the current year for three study sites were calculated. Table 2 lists stations and periods used in the analysis.

3.2.2. Monthly precipitation

The strongest July precipitation signal is observed at ALT (r=-0.54) and TAY (r=-0.51) with $\delta^{13}C$ chronologies ($p<0.05$). In addition, the ALT data shows a significant relationship ($p<0.05$) between March precipitation and TRW (r=0.37) and MXD (r=0.32), whereas April precipitation correlates positively with CWT (r=0.34). At YAK, July precipitation showed negative relationship with $\delta^{18}O$ in tree-ring cellulose (r=-0.34; $p<0.05$) only.

425 *3.2.3. Vapor pressure deficit (VPD)*

426 June VPD is significantly and positively correlated with the $\delta^{18}O$ chronology from ALT
427 (r=0.67 $p<0.05$, respectively) for the period 1950-2000. The $\delta^{13}C$ in tree-ring cellulose from
428 YAK correlate with July VPD only (r=0.69 $p<0.05$). We did not find significant influence of
429 VPD in TAY tree-ring and stable isotope parameters.

430

431 *3.2.4. Synthesis of the climate data analysis*

432 In summary, during the instrumental period of weather station observations (Table 2) summer
433 temperature impacts TRW, MXD and CWT at the high-latitude sites (YAK, TAY), while
434 summer precipitation affects stable carbon and oxygen isotopes (YAK, TAY, ALT), sunshine
435 duration (YAK, ALT), and vapor pressure deficit (YAK, ALT).

436

437 **3.3. Response of Siberian larch trees to climatic changes after the major volcanic erup-**
438 **tions**

439 Based on the statistical analysis above for the calibration period, we assumed that these rela-
440 tionships would not change over time and will provide information about climatic changes
441 during the past volcanic periods (Fig. 5).

442

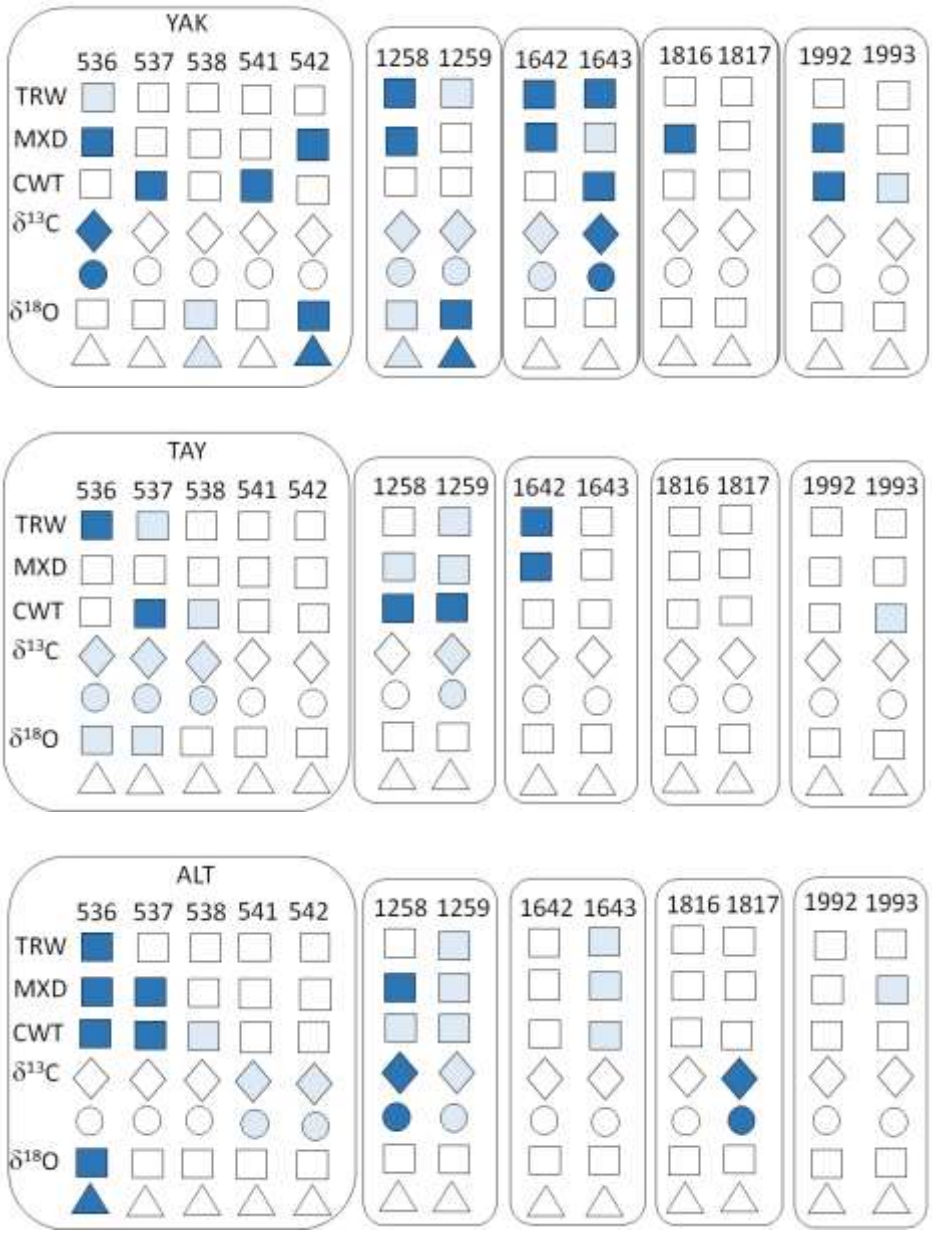

Fig. 5. Responses of larch trees from Yakutia (YAK), Taimyr (TAY) and Altai (ALT) to volcanic eruptions (Table 1). Squares, rhombs, circles, and triangles indicate the years following each eruption that can be considered as very extreme (negative values < 5th percentile of the PDFs, intensive color), extreme (negative values >5th, <10th percentile of the PDFs, light color) and non-extreme (>10th percentile of the PDFs, white color). July temperature changes are presented with squares. Summer vapor pressure deficit (VPD) variability is shown with circles. July precipitations are presented with rhombs, and July sunshine duration is shown as triangles.

457 *3.3.1. Temperature proxies*

458 We found strong negative summer air temperature anomalies at all sites after the CE 535 and
459 1257 volcanic eruptions. The temperature decrease was found in the TRW and CWT datasets
460 at all sites, and also in the MXD datasets at YAK and ALT (Fig. 5). For the volcanic erup-
461 tions in later centuries, the evidence for a decrease in temperature was not as pronounced.
462 Whereas no strong decline of summer temperature was found at ALT in CE 1642, we observe
463 a slight decrease in TRW, MXD and CWT values in 1643. By contrast, a cold summer was
464 recorded by most tree-ring parameters at YAK, except for $\delta^{18}O$. The absence of strong cool-
465 ing is even more so striking during the years that followed the CE 1815 Tambora eruption. In
466 CE 1816, only the MXD from YAK shows colder than normal conditions (Fig. 5). CE 1992
467 was recorded as a cold year in MXD and CWT from YAK, but again not at the other regions
468 and by other proxies.

469

470 *3.3.2. Moisture proxies: precipitation and VPD*

471 Based on the climatological analysis with the local weather stations data (Table 2, Fig. 4) for
472 all studied sites we considered $\delta^{13}C$ in tree-ring cellulose as a proxy for precipitation and va-
473 por pressure deficit changes. Yet, CWT from ALT could be considered as a proxy with mixed
474 temperature and precipitation signal (Fig. 4). Accordingly, the $\delta^{13}C$ values point to humid
475 summers at YAK in 536, 1258, 1259, 1642, and 1643, at TAY in 536-538, and 1259, and at
476 ALT the years of 541, 542, 1258, 1259 and 1817. Compared to other proxies and sites, the
477 years 536-538 were neither extremely humid nor dry at ALT (Fig. 5). No negative hydrologi-
478 cal anomalies were recorded after the Tambora and Pinatubo eruptions at the high-latitude
479 sites (YAK, TAY). However, positive anomalies were recorded in $\delta^{13}C$ values, pointing to
480 dry conditions at TAY in CE 1817 (Fig. 2). A rather wet summer was reconstructed for the

high-altitude ALT site in CE 1817 compared to 1816 (Fig. 5). Overall, there were mostly humid anomalies after the eruptions at YAK.

3.3.3. Sunshine duration proxies

Instrumental measurements of sunshine duration (Table 2) at YAK and ALT during the recent period showed a significant link with $\delta^{18}O$ cellulose. The sunshine duration is decreased after various eruptions at YAK (538, 542, 1258, and 1259) and in 536 at ALT site.

4. Discussion

In this paper, we analyze climatic anomalies in years following selected large volcanic eruptions using long-term tree-ring multi-proxy chronologies for $\delta^{13}C$ and $\delta^{18}O$, TRW, MXD, CWT for the high-latitude (YAK, TAY) and high-altitude (ALT) sites. Since trees as living organisms respond to various climatic impacts, the carbon assimilation and growth patterns accordingly leave unique "finger prints" in the photosynthates, which is recorded in the wood in the tree rings specifically and individually for each proxy.

4.1. Evaluation of the applied proxies in Siberian tree-ring data

This study clearly shows that each proxy has to be analyzed and interpreted specifically for its validity at each studied site and evaluated for its suitability for the reconstruction of abrupt climatic changes.

The TRW in temperature-limited environments is an indirect proxy for summer temperature reconstructions, as growth is a temperature-controlled process. Temperature clearly determines the duration of the growing season and the rate of cell division (Cuny et al., 2014). Accordingly, low temperature of growing season is recorded by narrow tree rings. The upper limit of temperature is specific to tree species and biome. In most cases, tree growth is limited

506 by drought rather than by high temperatures, since water shortage and VPD increase with in-
507 creasing temperature. Still this does not make TRW a suitable proxy to determine the influ-
508 ence of water availability and air humidity, especially at the temperature-limited sites.
509 MXD chronologies obtained for the Eurasian subarctic record mainly a July-August tempera-
510 ture signal (Vaganov et al., 1999; Sidorova et al., 2010; Büntgen et al., 2016) and add valua-
511 ble information about climate conditions toward the end of the growth season. Similarly,
512 CWT is an anatomical parameter, which contains information on carbon sink limitation of the
513 cambium due to extreme cold conditions (Panyushkina et al., 2003; Fonti et al., 2013; Bryu-
514 khanova et al., 2015). There is a strong signal of low cell number within a growing season, for
515 example, strong decreasing CWT in CE 537 at YAK or the formation of frost rings at ALT in
516 (CE 536-538, and 1259) has been shown in our study.
517 Low $\delta^{13}C$ values can be explained by a reduction in photosynthesis caused by volcanic dust
518 veils. For the distinction whether $\delta^{13}C$ is predominantly determined by A_N or g_l the combined
519 evaluation with $\delta^{18}O$ or TRW is needed. High $\delta^{18}O$ values indicate high VPD, which induces
520 a reduction in stomatal conductance, reducing the back diffusion of depleted water molecules
521 from the ambient air. This confirms a sunny CE 1993 at ALT with mild weather conditions
522 according to observational data from the closest weather station (Table 2). Interestingly, we
523 also find less negative values for $\delta^{13}C$ in the same period. This shows that the two isotopes
524 correlate with each other and indicates the need for a combined evaluation of the C and O iso-
525 topes (Scheidegger et al., 2000) taking into account precautions as suggested by Roden and
526 Siegwolf (2012).
527

528 *4.2. Lag between volcanic events and response in tree rings*

529 Most discussed events suggest a lag between the eruption and the tree-ring response for one
530 year or more (Fig. 3). This lag is explained by the tree's use of stored carbohydrates, which

531 are the substrate for needle and early wood production. These stored carbohydrates carry the
532 isotopic signal of previous years and depend on their remobilization, as such the signals may
533 be masked in freshly produced biomass. The delayed signal could also reflect the time needed
534 for the dust veil to be transported to the study regions.
535
536 *4.3. Temperature and sunshine duration changes after stratospheric volcanic eruptions*
537 Correlation functions show that MXD and CWT (with the exception of TAY in the latter
538 case), and to a lesser extent TRW chronologies, portray the strongest signals for summer
539 (June-August) temperatures. In addition, significant information about sunshine duration can
540 be derived from the YAK and ALT $\delta^{18}O$ series. Thus, we hypothesize that extremely narrow
541 TRW and very negative anomalies observed in the MXD and CWT chronologies of YAK and
542 to a lesser extent at ALT, along with low $\delta^{18}O$ values reflect cold and low sunshine duration
543 conditions in summer. Presumably, the temperatures were below the threshold values for
544 growth over much of the growing season (Körner, 2015). This hypothesis of a generalized re-
545 gional cooling after both eruptions is further confirmed by the occurrence of frost rings at
546 ALT site in CE 538, 1259 (Myglan et al., 2008; Guillet et al., 2017), as well as in neighboring
547 Mongolia (D'Arrigo et al., 2001). The unusual cooling in CE 536-542 is also evidenced by a
548 very small number of cells formed at YAK (Churakova (Sidorova) et al., 2014). Although
549 $\delta^{18}O$ is an indirect proxy for needle temperature, low $\delta^{18}O$ values in CE 538, 542, 1258, and
550 1259 for YAK and in CE 536 for ALT are a result of low irradiation, leading to low tempera-
551 ture and low VPD (high stomatal conductance), both likely a result from volcanic dust veils.
552 Similarly, in the aftermath of the Samalas eruption, the persistence of summer cooling is lim-
553 ited to CE 1258 and 1259 at the three studied sites, which is in line with findings of Guillet et

554 al., (2017). Interestingly, a slight decrease in oxygen isotope chronologies, which can be re-
555 lated to low levels of summer sunshine duration (i.e. low leaf temperatures), allows for hy-
556 pothesizing that cool conditions could have prevailed.
557 For all later high-magnitude CE eruptions, temperature-sensitive tree-ring proxies do not evi-
558 dence a generalized decrease in summer temperatures. Paradoxically, the impacts of the Tam-
559 bora eruption, known for its triggering of a widespread "year without summer" (Harrington,
560 1992), did only induce abnormal MXD at YAK in 1816, but no anomalies are observed at
561 TAY and ALT, except for the positive deviation of $\delta^{13}C$ at TAY and the negative anomaly at
562 ALT in CE 1817 (Fig. 2, Fig. 5, Fig. S1). While these findings may seem surprising, they are
563 in line with the TRW and MXD reconstructions of Briffa et al. (1998) or Guillet et al. (2017),
564 who found limited impacts of the CE 1815 Tambora eruption in Eastern Siberia and Alaska
565 using TRW and MXD data only. The inclusion of CWT chronologies by Barinov et al. (2018)
566 confirms the absence of a significant cooling signal after the second largest eruption of the
567 last millennium (CE 1815) in larch trees of the Altai-Sayan mountain region.
568 Finally, in CE 1992, our results evidence cold conditions at YAK, which is consistent with
569 weather observations showing that the below-average anomalies of summer temperatures (af-
570 ter Pinatubo eruption) were indeed limited to Northeastern Siberia (Robock, 2000). As both
571 isotopes indicate a reduction in stomatal conductance, we found that warm (in agreement with
572 MXD and CWT) and dry conditions were prevalent at ALT at this time. This isotopic constel-
573 lation was confirmed by the positive relationships between VPD and $\delta^{18}O$ and $\delta^{13}C$ at ALT.
574 However, temperature and sunshine duration are not always highly coherent over time due to
575 the influence of other factors, like Arctic Oscillations as suggested for Fennoscandia regions
576 by Loader et al. (2013).
577
578 *4.4. Moisture changes*

579 Water availability is a key parameter for Siberian trees as they are growing under extremely
580 continental conditions with hot summers and cold winters, and even more so with very low
581 annual precipitation (Table 2). Permafrost plays a crucial role and can be considered as a
582 buffer for additional water sources during hot summers (Sugimoto et al., 2002; Boike et al.,
583 2013; Saurer et al., 2016). Yet, thawed permafrost water is not always available to roots due
584 to the surficial structure of the root plate or extremely cold water temperature (close to 0ºC),
585 which can hardly be utilized by trees (Churakova (Sidorova) et al., 2016). Thus, Siberian trees
586 are highly susceptible to drought, induced by dry and warm air during July and therefore the
587 stable carbon isotopes can be sensitive indicators of such conditions. After volcanic eruptions,
588 however, low light intensity due to dust veils induce low temperatures and reduced VPD, the
589 driver for evapotranspiration. Under such conditions drought stress is unlikely to occur. How-
590 ever, the transition phases with changes from cool and moist to warm and dry conditions are
591 more critical when drought is more likely to occur.
592 In our study, higher $\delta^{13}C$ values in tree-ring cellulose indicate increasing drought conditions
593 as a consequence of reduced precipitation for two years after the CE 1815 volcanic eruption at
594 TAY site. No further extreme hydro-climatic anomalies occurred at Siberian sites in the after-
595 math of the Pinatubo eruption.
596
597 *4.5. Synthetized interpretation from the multi-parameter tree-ring proxies*
598 Our analysis demonstrates the added value of a tree-ring derived multi-proxy approach to bet-
599 ter capture the climatic variability after large volcanic eruptions. Besides the well-documented
600 effects of temperature derived from TRW and MXD, CWT, stable carbon and oxygen iso-
601 topes in tree-ring cellulose provide important and complementary information about moisture
602 and sunshine duration changes (an indirect proxy for leaf temperature effective for air-to-leaf
603 VPD) after stratospheric volcanic eruptions.

Our results reveal the complex behavior of the Siberian climatic system to the stratospheric volcanic eruptions of the Common Era. The CE 535 and CE 1257 Samalas eruptions caused substantial cooling – very likely induced by dust veils (Churakova (Sidorova) et al., 2014; Guillet et al., 2017; Helama et al., 2018) – as well as humid conditions at both the high-latitude and high-altitude sites. Conversely, only local and limited climate responses were observed after the CE 1641 Parker, 1815 Tambora, and 1991 Pinatubo eruptions. Similar site-dependent impacts referred to the coldest summers of the last millennium in the Northern Hemisphere based on TRW and MXD reconstructions (Schneider et al., 2015; Stoffel et al., 2015; Wilson et al., 2016; Guillet et al., 2017). This absence of widespread and intense cooling or missing drastic changes in hydrological regime over vast regions of Siberia may result from the location and strength of the volcanic eruption, atmospheric transmissivity as well as from the modulation of radiative forcing effects by regional climate variability. These results are consistent with other regional studies, which interpreted the spatial-temporal heterogeneity of tree responses to past volcanic events (Wiles et al., 2014; Esper et al., 2017; Barinov et al., 2018) in terms of regional climates.

5. Conclusions

In this study, we demonstrate that the consequences of large volcanic eruptions on climate are rather complex between sites and among events. The different locations and magnitudes of eruptions, but also regional climate variability, may explain some of this heterogeneity. We show that each tree-ring and isotope proxy alone cannot provide the full information of the volcanic impact on climate, but that they, when combined, contribute to the formation of the full picture, which is critical for a comprehensive description of climate dynamics induced by volcanism and the inclusion of these phenomena in global climate models.

628 The analyses with a larger number of samples in the investigations of Siberian and other
629 Northern Hemispheric sites will indeed to provide higher certainty in terms of data interpreta-
630 tion of climatic dynamics of these boreal regions. However, the multi-proxy approach as ap-
631 plied in our study also provides a strong set of complementary information to the research
632 field, as it allows the refinement of the interpretations and thus improves our understanding of
633 the heterogeneity of climatic signals after CE stratospheric volcanic eruptions, as recorded in
634 multiple tree-ring and stable isotope parameters.
635
636 **Author contribution:** TRW analysis was performed at V.N. Sukachev Institute of Forest SB
637 RAS by O.V. Churakova (Sidorova), D.V. Ovchinnikov, V.S. Myglan and O.V. Naumova.
638 CWT analysis was carried out at the V. N. Sukachev Institute of Forest SB RAS, Krasno-
639 yarsk, Russia by M.V. Fonti and at the University of Arizona by I.P. Panyushkina. Stable iso-
640 tope analysis was conducted at the Paul Scherrer Institute (PSI), by O.V. Churakova (Si-
641 dorova), M. Saurer, and R. Siegwolf. MXD measurements were realized with a DENDRO
642 Walesh 2003 densitometer at WSL and at the V.N. Sukachev Institute of Forest SB RAS,
643 Krasnoyarsk, Russia by O.V. Churakova (Sidorova) and A.V. Kirdyanov. Samples from YAK
644 and TAY were collected by M.M. Naurzbaev. All authors contributed significantly to the data
645 analysis and paper writing.
646
647 **Acknowledgements:** This work was supported by Marie Curie International Incoming Fel-
648 lowship [EU_ISOTREC 235122], Re-Integration Marie Curie Fellowship [909122] and UFZ
649 scholarship [2006], RFBR [09-05-98015_r_sibir_a] granted to Olga V. Churakova (Si-
650 dorova); SNSF Matthias Saurer [200021_121838/1]; Era.Net RusPlus project granted to
651 Markus Stoffel [SNF IZRPZ0_164735] and RFBR [№ 16-55-76012 Era_a] granted to Eugene
652 A. Vaganov; project granted to Vladimir S. Myglan RNF, Russian Scientific Fond [№ 15-14-

30011]; Alexander V. Kirdyanov was supported by the Ministry of Education and Science of the Russian Federation [#5.3508.2017/4.6] and RSF [#14-14-00295]; Scientific School [3297.2014.4] granted to Eugene A. Vaganov; and US National Science Foundation (NSF) grants [#9413327, #970966, #0308525] to Malcolm K. Hughes and US CRDF grant # RC1-279, to Malcolm K. Hughes and Eugene A. Vaganov. We thank Tatjana Boettger for her support and access to the stable isotope facilities within UFZ Haale/Saale scholarship 2006; Anne Verstege, Daniel Nievergelt for their help with sample preparation for the MXD and Paolo Cherubini for providing lab access at the Swiss Federal Institute for Forest, Snow and Landscape Research (WSL).

We thank two anonymous reviewers and handling Editor Juerg Luterbacher for their constructive comments on this manuscript.

664 **Figure legends**

665

666 **Fig. 1.** Location of the study sites (stars) and known volcanos from the tropics (black dots)
667 considered in this study (a). Annual tree-ring width index (light lines) and smoothed by 51-
668 year Hamming window (bold lines) from the northeastern Yakutia (YAK - **blue**, b) (Hughes
669 et al., 1999; Sidorova and Naurzbaev 2002; Sidorova 2003), eastern Taimyr (TAY - **green**, c)
670 (Naurzbaev et al., 2002), and Russian Altai (ALT - **red**, d) (Myglan et al., 2009). Photos show
671 the larch stnads at YAK, TAY (M.M. Naurzbaev) and ALT (V.S. Myglan) sites.

672

673 **Fig. 2.** Normalized (z-score) individual tree-ring index chronologies (TRW, **black**), maxi-
674 mum latewood density (MXD, **purple**), cell wall thickness (CWT, **green**), $\delta^{13}C$ (**red**) and
675 $\delta^{18}O$ (**blue**) in tree-ring cellulose chronologies from northeastern Yakutia (YAK), eastern Tai-
676 myr (TAY) and Altai (ALT) for the specific periods 520-560, 1242-1286, 1625-1660, 1790-
677 1835, 1950-2000 before and after the eruptions CE 535, 540, 1257, 1640, 1815 and 1991 are
678 presented. Vertical lines show year of the eruptions.

679

680 **Fig. 3.** Superposed epoch analysis (SEA) of $\delta^{18}O$, $\delta^{13}C$, CWT, TRW, and MXD chronologies
681 for the Yakutia (YAK), Taimyr (TAY), and Altai (ALT) sites, summarizing negative anoma-
682 lies 15 years before and 20 years after the volcanic eruptions in CE 535, 540, 1257, 1640,
683 1815, and 1991. Statistically negative anomalies are marked with a red star (*$p<0.05$).

684

685 **Fig. 4.** Significant correlation coefficients between tree-ring parameters: TRW, MXD, CWT,
686 $\delta^{13}C$ and $\delta^{18}O$ versus weather station data: temperature (T, red), precipitation (P, blue), vapor

687 pressure deficit (VPD, green), and sunshine duration (S, yellow) from September of the previ-
688 ous year to August of the current year for three study sites were calculated. Table 2 lists sta-
689 tions and periods used in the analysis.
690
691 **Fig. 5.** Responses of larch trees from Yakutia (YAK), Taimyr (TAY) and Altai (ALT) to vol-
692 canic eruptions (Table 1). Squares, rhombs, circles, and triangles indicate the years following
693 each eruption that can be considered as very extreme (negative values < 5th percentile of the
694 PDFs, intensive color), extreme (negative values >5th, <10th percentile of the PDFs, light
695 color) and non-extreme (>10th percentile of the PDFs, white color). July temperature changes
696 are presented with squares. Summer vapor pressure deficit (VPD) variability is shown with
697 circles. July precipitations are presented with rhombs, and July sunshine duration is shown as
698 triangles.
699
700 **Table 1.** List of stratospheric volcanic eruptions used in the study
701
702 **Table 2.** Tree-ring sites in northeastern Yakutia (YAK), eastern Taimyr (TAY), and Altai
703 (ALT) and weather stations used in the study. Monthly air temperature (T, °C), precipitation
704 (P, mm), sunshine duration (S, h/month) and vapor pressure deficit (VPD, kPa) data were
705 downloaded from the meteorological database: http://aisori.meteo.ru/ClimateR.
706
707 **Fig. S1.** Probability density function (Pdf) computed for each of the tree-ring parameter for
708 northeastern Yakutia (YAK), eastern Taimyr (TAY) and Russian Altai (ALT). Tree-ring pa-
709 rameters (TRWi - **black**, MXD – **purple**, CWT – **green**, $\delta^{18}O$ - **blue** and $\delta^{13}C$ - **red**) in bold
710 lines represent the probability density function. Dotted lines represent the anomalies (z-score)

711 observed for the first and second years following the CE 535, 540, 1257, 1640, 1815 and 1991
712 volcanic eruptions for each tree-ring parameter.
713

714 **References**

715 Abaimov, A.P., Bondarev, A.I., Yzrzanova, O.V., Shitova, S.A.: Polar forests of Krasnoyarsk
716 region. Nauka Press, Novosibirsk. 208 p, 1997.
717 Battipaglia, G., Cherubini, P., Saurer, M., Siegwolf, R.T.W., Strumia, S., Cotrufo, M.F.: Vol-
718 canic explosive eruptions of the Vesuvio decrease tree-ring growth but not photosyn-
719 thetic rates in the surrounding forests. Global Change Biology. 13, 1-16, 2007.
720 Barinov, V.V., Myglan, V.S., Taynik, A.V., Ojdupaa, O.Ch., Agatova, A.R., Churakova (Si-
721 dorova) O.V.: Extreme climatic events in Altai-Sayan region as indicator of major
722 volcanic eruptions. Geophysical processes and biosphere. 17, 45-61, 2018. doi:
723 10.21455/GPB2018.3-3.
724 Boettger T., Haupt, M., Knöller, K., Weise, S., Waterhouse, G.S. … Schleser, G.H.: Wood
725 cellulose preparation methods and mass spectrometric analyses of $\delta^{13}C$, $\delta^{18}O$, and
726 non ex-changeable $\delta^{2}H$ values in cellulose, sugar, and starch: An inter-laboratory
727 comparison. Anal. Chem. 79, 4603–4612, doi:10.1021/ac0700023, 2007.
728 Boike, J., Kattenstroth, B., Abramova, K., Bornemann, N., Cherverova, A., Fedorova, I.,
729 Fröb, K., Grigoriev, M., Grüber, M., Kutzbach, L., Langer, M., Minke, M., Muster,
730 S., Piel, K., Pfeiffer, E.-M., Stoff, G., Westermann, S., Wischnewski, K., Wille, C.,
731 Hubberten, H.-W.: Baseline characteristics of climate, permafrost and land cover
732 from a new permafrost observatory in the Lena Rive Delta, Siberia (1998-2011). Bi-
733 ogeosciences. 10, 2105-2128, 2013.
734 Briffa, K.R., Jones, P.D., Schweingruber, F.H., Osborn, T.J.: Influence of volcanic eruptions
735 on Northern Hemisphere summer temperature over the past 600 years. Nature. 393,
736 450–455, 1998.
737 Bryukhanova, M.V., Fonti, P., Kirdyanov, A.V., Siegwolf, R., Saurer, M., Pochebyt, N.P.,
738 Churakova (Sidorova), O.V., Prokushkin, A.S.: The response of $\delta^{13}C$, $\delta^{18}O$ and cell

739 anatomy of *Larix gmelinii* tree rings to differing soil active layer depths. Dendro-
740 chronologia. 34, 51-59, 2015.

741 Büntgen, U., Myglan, V.S., Ljungqvist, F.C., McCormick, M., Di Cosmo, N., Sigl M., ….Kir-
742 dyanov, A.V.: Cooling and societal change during the Late Antique Little Ice Age
743 from 536 to around 660 AD. Nature Geoscience. 9, 231-236, 2016.

744 Castagneri, D., Fonti, P., von Arx, G., Carrer, M.: How does climate influence xylem mor-
745 phogenesis over the growing season? Insights from long-term intra-ring anatomy in
746 *Picea abies*. Annals of Botany. 19, 1011-1020, doi:10.1093/aob/mcw274, 2017.

747 Cernusak, L., Ubierna, N., Winter, K., Holtum, J.A.M., Marshall, J.D., Farquhar, G.D.: Envi-
748 ronmental and physiological determinants of carbon isotope discrimination in terres-
749 trial Plants. Transley Review New Phytologist. 200, 950-965, 2013.

750 Cernusak, L., Barbour, M., Arndt, S., Cheesman, A., English, N., Field, T., Helliker, B., Hol-
751 loway-Phillips, M., Holtum, J., Kahmen, A., Mcnerney F, Munksgaard N, Simonin
752 K, Song X, Stuart-Williams H, West J and Farquhar G.: Stable isotopes in leaf water
753 of terrestrial plants. Plant, Cell & Environment. 39 (5), 1087-1102, 2016.

754 Churakova (Sidorova), O.V., Bryukhanova, M., Saurer, M., Boettger, T., Naurzbaev, M.,
755 Myglan, V.S., Vaganov, E.A., Hughes, M.K., Siegwolf, R.T.W.: A cluster of strato-
756 spheric volcanic eruptions in the AD 530s recorded in Siberian tree rings. Global and
757 Planetary Change. 122, 140-150, 2014.

758 Churakova (Sidorova), O.V., Shashkin, A.V., Siegwolf, R., Spahni, R., Launois, T., Saurer
759 M., Bryukhanova, M.V., Benkova, A.V., Kupzova, A.V., Vaganov, E.A., Peylin, P.,

760 Masson-Delmotte, V., Roden, J.: Application of eco-physiological models to the cli-
761 matic interpretation of $\delta^{13}C$ and $\delta^{18}O$ measured in Siberian larch tree-rings. Dendro-
762 chronologa, doi:10.1016/j.dendro.2015.12.008, 2016.
763 Cook, E., Briffa, K., Shiyatov, S., Mazepa, V.: Tree-ring standardization and growth trend es-
764 timation. In: Methods of dendrochronology: applications in the environmental sci-
765 ences, Eds: Cook, E.R., Kairiukstis, L.A. 104-123, 1990.
766 Cook, E.R., Krusic, P.J.: A Tree-Ring Standardization Program Based on De-trending and
767 Autoregressive Time Series Modeling, with Interactive Graphics (ARSTAN). (Ed.
768 by E.R., Cook and P.J., Krusic), 2008.
769 Craig, H.: Isotopic variations in meteoric waters. Science. 133, 1702– 1703, 1961.
770 Crowley, T.J., Unterman, M.B.: Technical details concerning development of a 1200 yr.
771 proxy index for global volcanism. Earth Syst. Sci. Data. 5, 187-197, 2013.
772 Cuny, H.E., Rathgeber, C.B.K., Frank, D., Fonti, P., Fournier, M.: Kinetics of tracheid devel-
773 opment explain conifer tree-ring structure. New Phytologist. 203, 1231–1241, 2014.
774 D'Arrigo, R.D., Jacoby, G.C., Frank, D., Pederson, N.D., Cook, E., Buckly, B.M., Nachin, B.,
775 Mijidorj, R., Dugarjav, C.: 1738-years of Mongolian temperature variability inferred
776 from a tree-ring width chronology of Siberian pine. Geophisycal Research Letters.
777 Vol. 28 (3), 543-546, 2001.
778 Dansgaard, W.: Stable isotopes in precipitation. Tellus. 16, 436–468, 1964.
779 Dawson, T.E., Mambelli, S., Plamboeck, A.H., Templer, P.H., Tu, K.P.: Stable isotopes in
780 plant ecology Ann. Review of Ecology and Systematics. 33, 507-559, 2004.
781 Dongmann, G., Förstel, H., Wagener, K.: ^{18}O-rich oxygen from land photosynthesis. Nature
782 New Biol. 240, 127–128, 1972.

783 Eschbach, W., Nogler, P., Schär, E., Schweingruber, F.H.: Technical advances in the radi-
784 odensitometrical determination of wood density. Dendrochronologia. 13, 155–168,
785 2015.
786 Esper, J., Büntgen, U., Hartl-Meier, C., Oppenheimer, C., Schneider, L.: Northern Hemi-
787 sphere temperature anomalies during 1450s period of ambiguous volcanic forcing.
788 Bull. Volcanology. 79, 41, 2017.
789 Esper, J., St. George, S., Anchukaitis, K., D'Arrigo, R., Ljungqvist, F., Luterbacher, J.,
790 Schneider, L., Stoffel, M., Wilson, R., Büntgen, U.: Large-scale, millennial-length
791 temperature reconstructions from tree-rings. Dendrochronologia. 50, 81–90, 2018.
792 Farquhar, G. D.: Eds. Stable Isotopes and Plant Carbon-Water Relations. Academic Press,
793 San Diego. 47–70, 1982.
794 Farquhar, G.D., Ehleringer, J.R., Hubick, K.T.: Annu. Rev. Plant Physiol. Plant Mol. Biol. 40,
795 503 p, 1989.
796 Farquhar, G.D., Lloyd, J.: Carbon and oxygen isotope effects in the exchange of carbon diox-
797 ide between terrestrial plants and the atmosphere. In: Ehleringer, J.R., Hall, A.E.,
798 Farquhar, G.D. (Eds) Stable Isotopes and Plant Carbon-Water Relations. Academic
799 Press, San Diego, 47–70, 1993.
800 Fonti, P., Bryukhanova, M.V., Myglan, V.S., Kirdyanov, A.V., Naumova, O.V., Vaganov,
801 E.A.: Temperature-induced responses of xylem structure of *Larix sibirica* (Pinaceae)
802 from Russian Altay. American Journal of Botany. 100 (7), 1-12, 2013.
803 Francey, R.J., Allison, C.E., Etheridge D.M., Trudinger, C.M., Langenfelds, R.L., Michel, E.,
804 Steele, L.P.: A 1000-year high precision record of $\delta^{13}C$ in atmospheric CO_2. Tellus.
805 Ser. B (51), 170-193, 1999.
806 Fritts, H.C.: Tree-rings and climate. London. New York; San Francisco: Acad. Press. 567 p,
807 1976.

808 Furst, G.G.: Methods of Anatomical and Histochemical Research of Plant Tissue. Nauka,
809 Moscow. 156 p, 1979.
810 Gao, C., Robock, A., Ammann, C.: Volcanic forcing of climate over the past 1500 years: An
811 improved ice core-based index for climate models. J. Geophys. Res. Atmos.
812 113:D23111. doi:10.1029/2008jd010239, 2008.
813 Gennaretti, F., Huard, D., Naulier, M., Savard, M., Bégin, C., Arseneault, D., Guiot, J.:
814 Bayesian multiproxy temperature reconstruction with black spruce ring widths and
815 stable isotopes from the northern Quebec taiga. Clym. Dyn. doi: 10.1007/s00382-
816 017-3565-5, 2017.
817 Gillett, N.P., Weaver, A.J., Zwiers, F.W. Wehner, M.F.: Detection of volcanic influence on
818 global precipitation. Geophysical Research Letters. 31 (12),
819 doi:10.1029/2004GL020044 R, 2004.
820 Groisman, P.Ya.: Possible regional climate consequences of the Pinatubo eruption. Geophys.
821 Res. Lett., 19, 1603–1606, 1992.
822 Gu, L., Baldocchi, D.D., Wofsy, S.C., Munger, J.W., Michalsky, J.J., Urbanski, S.P., Boden,
823 T.A.: Response of a deciduous forest to the Mount Pinatubo eruption: Enhanced pho-
824 tosynthesis, Science. 299 (5615), 2035–2038, 2003.
825 Guillet, S., Corona, C., Stoffel, M., Khodri M., Lavigne F., Ortega, P.,….Oppenheimer, C.:
826 Climate response to the 1257 Samalas eruption revealed by proxy records. Nature
827 geoscience, doi:10.1038/ngeo2875, 2017.
828 Hansen, J., Sato, M., Ruedy, R., Lacis, A., Asamoah, K., Borenstein S,, ….Wilson, H.: A
829 Pinatubo climate modeling investigation. In The Mount Pinatubo Eruption: Effects
830 on the Atmosphere and Climate, NATO ASI Series Vol. I 42. G. Fiocco, D. Fua, and
831 G. Visconti, Eds. Springer-Verlag, 233-272, 1996.

Harrington, C.R.: The Year without a summer? World climate in 1816. Ottawa: Canadian Museum of Nature, ISBN 0660130637, 1992.

Helama, S., Arppe, L., Uusitalo, J., Holopainen, J., Mäkelä, H.M., Mäkinen, H., Mielikäinen, K., Nöjd, P., Sutinen, R., Taavitsainen, J.-P., Timonen, M., Oinonen, M.: Volcanic dust veils from sixth century tree-ring isotopes linked to reduced irradiance, primary production and human health. Scientific reports 8, 1339, doi:10.1038/s41598-018-19760-w, 2018.

Hughes, M.K., Vaganov, E.A., Shiyatov, S.G., Touchan, R. & Funkhouser, G.: Twentieth-century summer warmth in northern Yakutia in a 600-year context. The Holocene. 9(5), 603-608, 1999.

Iles, C.E., Hegerl, G.C.: The global precipitation response to volcanic eruptions in the CMIP5 models. Environ. Res. Lett. 9, doi:10.1088/1748-9326/9/10/104012, 2014.

Joseph, R., Zeng, N.: Seasonally modulated tropical drought induced by volcanic aerosol. J. Climate, 24, 2045–2060, 2011.

Kirdyanov, A.V., Treydte, K.S., Nikolaev, A., Helle, G., Schleser, G.H.: Climate signals in tree-ring width, wood density and $\delta^{13}C$ from larches in Eastern Siberia (Russia) Chemical Geology, 252, 31-41, 2008. doi:10.1016/j.chemgeo.2008.01.023

Körner, Ch.: Paradigm shift in plant growth control. Curr. Opinion Plant Biol. 25, 107-114, 2015.

Lavigne, F., Degeai, J.-P., Komorowski, J.-C., Guillet, S., Robert, V., Lahitte, P., Oppenheimer, C., Stoffel, M., Vidal, C.M., Suro, I.P., Wassmer, P., Hajdas, I., Hadmoko, D.S., Belizal, E.: Source of the great A.D. 1257 mystery eruption unveiled, Samalas volcano, Rinjani Volcanic Complex, Indonesia. Proc Natl Acad Sci 110, 16742–16747, doi:10.1073/pnas.1307520110, 2013.

856 Lenz, O., Schär, E., Schweingruber F.H.: Methodische Probleme bei der radiographisch-den-
857 sitometrischen Bestimmung der Dichte und der Jahrrinbreiten von Holz.
858 Holzforschung, 30, 114-123, 1976.
859 Loader, N.J., Robertson, I., Barker, A.C., Switsur, V.R., Waterhouse, J.S.: Improved tech-
860 nique for the batch processing of small whole wood samples to alpha-cellulose.
861 Chemical Geology. 136, 313-317, 1997.
862 Loader, N.J., Young, G.H.F., Grudd, H., McCarroll.: Stable carbon isotopes from Torneträsk,
863 norther Sweden provide a millennial length reconstruction of summer sunshine and
864 its relationship to Arctic circulation. Quaternary Science Reviews. 62, 97-113, 2013.
865 McCarroll, D., Loader, N.J.: Stable isotopes in tree rings. Quaternary Science Review. 23,
866 771-801, 2004.
867 Meronen, H., Henriksson, S.V., Räisänen, P., Laaksonen, A.: Climate effects of northern
868 hemisphere volcanic eruptions in an Earth System Model. Atmospheric Research,
869 114-115: 107-118, 2012.
870 Munro, M.A.R., Brown, P.M., Hughes, M.K., Garcia, E.M.R.: Image analysis of tracheid
871 dimensions for dendrochronological use. Radiocarbon, Eds. by M.D. Dean, J.
872 Swetnam T), pp. 843-851. Tucson, Arizona, 1996.
873 Myglan, V.S., Oidupaa, O. Ch., Kirdyanov, A.V., Vaganov, E.A.: 1929-year tree-ring chro-
874 nology for Altai-Sayan region (Western Tuva). Journal of archeology, ethnography
875 and anthropology of Eurasia. 4 (36), 25-31, 2008.
876 Naurzbaev, M.M., Vaganov, E.A., Sidorova, O.V., Schweingruber, F.H.: Summer tempera-
877 tures in eastern Taimyr inferred from a 2427-year late-Holocene tree-ring chronology
878 and earlier floating series. The Holocene. 12(6), 727-736, 2002.

879 Panofsky, H.A., Brier, G.W.: Some applications of statistics to meteorology. University Park,
880 PA. Mineral industries extension services, college of mineral industries, Pennsylva-
881 nia State University, 224 p, 1958.
882 Panyushkina, I.P., Hughes, M.K., Vaganov, E.A., Munro, M.A.R.: Summer temperature in
883 northern Yakutia since AD 1642 reconstructed from radial dimensions of larch tra-
884 cheids. Canadian Journal of Forest Research. 33, 1-10, 2003.
885 Peng, Y., Shen, C., Wang, W.-C., Xu, Y.: Response of summer precipitation over Eastern
886 China to large volcanic eruptions. Journal of Climate. 23, 818-824, 2009.
887 R Core Team.: R: A Language and Environment for Statistical Computing. Vienna, Austria,
888 2016.
889 Robock, A.: Volcanic eruptions and climate. Reviews of Geophysics. 38(2), 191-219, 2000.
890 Robock, A., Liu, Y.: The volcanic signal in Goddard Institute for Space Studies three-imen-
891 sional model simulations. J. Climate. 7, 44-55, 1994.
892 Roden, J.S., Siegwolf, R: Is the dual isotope conceptual model fully operational? Tree Physi-
893 ology. 32, 1179-1182, 2012.
894 Saurer, M., Robertson, I., Siegwolf, R., Leuenberger, M.: Oxygen isotope analysis of
895 cellulose: an interlaboratory comparison. Analytical cemistry, 70, 2074-2080, 1998.
896 Saurer, M., Kirdyanov, A. V., Prokushkin, A. S., Rinne, K. T., Siegwolf, R.T.W.: The impact
897 of an inverse climate-isotope relationship in soil water on the oxygen-isotope
898 composition of *Larix gmelinii* in Siberia. New Phytologist. 209(3), 955-964, 2016.
899 Scheidegger, Y., Saurer, M., Bahn, M., Siegwolf, R.: Linking stable oxygen and carbon iso-
900 topes with stomatal conductance and photosynthetic capacity: a conceptual model.
901 Oecologia. 125, 350–357. doi: 10.1007/s004420000466, 2000.
902 Schneider, L., Smerdon, J.E., Büntgen, U., Wilson, R.J.S., Myglan, V.S., Kirdyanov, A.V.,
903 Esper, J.: Revising mid-latitude summer temperatures back to A.D. 600 based on a

wood density network. Geophys. Res. Lett. 42, GL063956, doi:10.1002/2015gl063956, 2015.

Schweingruber, F.H.: Tree rings and environment dendroecology. Paul Haupt Publ Bern, Stuttgart, Vienna 1996. pp. 609, 1996.

Sidorova, O.V., Naurzbaev, M.M.: Response of *Larix cajanderi* to climatic changes at the upper timberline and in the Indigirka River valley. Lesovedenie (in Russian). 2, 73-75, 2002.

Sidorova, O.V.: Long-term climatic changes and the larch radial growth on the northern Middle Siberia and the Northeastern Yakutia in the Late Holocene. Abs. PHD Diss, V.N. Sukachev Institute of Forest, Krasnoyarsk, 2003.

Sidorova, O.V., Naurzbaev, M.M., Vaganov, E.A.: Response of tree-ring chronologies growing on the Northern Eurasia to powerful volcanic eruptions. Problems of ecological monitoring and ecosystem modeling, XX, 60-72, 2005.

Sidorova, O.V., Saurer, M., Myglan, V.S., Eichler, A., Schwikowski, M., Kirdyanov, A.V., Bryukhanova, M.V., Gerasimova, O.V., Kalugin, I., Daryin, A., Siegwolf, R.: A multi-proxy approach for revealing recent climatic changes in the Russian Altai. Climate Dynamics, 38 (1-2), 175–188, 2011.

Sidorova, O.V., Siegwolf, R., Myglan, V.S., Loader, N.J., Helle, G., Saurer, M.: The application of tree-rings and stable isotopes for reconstructions of climate conditions in the Altai-Sayan Mountain region. Climatic Changes, doi: 10.1007/s10584-013-0805-5, 2012.

Sidorova, O.V., Siegwolf, R., Saurer, M., Naurzbaev, M., Shashkin, A.V., Vaganov, E.A.: Spatial patterns of climatic changes in the Eurasian north reflected in Siberian larch tree-ring parameters and stable isotopes. Global Change Biology, doi: 10.1111/j.1365-2486.2009.02008.x, 16, 1003-1018, 2010.

Sidorova, O.V., Siegwolf, R.T.W., Saurer, M., Naurzbaev, M.M., Vaganov, E.A.: Isotopic composition ($\delta^{13}C$, $\delta^{18}O$) in Siberian tree-ring chronology. Geophysical research Biogeosciences. 113, 1-13, 2008.

Sigl, M., Winstrup, M., McConnell, J.R.: Timing and climate forcing of volcanic eruptions for the past 2500 years. Nature. 523, 543-549. doi:10.1038/nature14565, 2015.

Sprenger, M., Tetzlaff, D., Buttle, J. M., Laudon, H., Leistert, H., Mitchell, C., Snelgrove, J., Weiler, M., Soulsby, C.: Measuring and modelling stable isotopes of mobile and bulk soil water, Vadose Zone Journal, https://doi.org/10.2136/vzj2017.08.0149, 20, 2017.

Sternberg, L.S.O.: Oxygen stable isotope ratios of tree-ring cellulose: The next phase of understanding. New Phytologist. 181 (3), 553-562, 2009.

Stirzaker, D.: Elementary Probability density functions. Cambridge. Sec. Ed. 538 p, 2003.

Stoffel, M., Khodri, M., Corona, C., Guillet, S., Poulain, V., Bekki, S., Guiot, J., Luckman, B.H., Oppenheimer, C., Lebas, N., Beniston, M., Masson-Delmotte, V.: Estimates of volcanic-induced cooling in the Northern Hemisphere over the past 1500 years. Nature Geoscience. 8, 784–788, 2015.

Stothers, R.B.: Climatic and Demographic Consequences of the Massive Volcanic Eruption of 1258. Climatic Change. 45, 361-374, 2000.

Stothers, R.B.: Mystery cloud of AD 536. Nature. 307, 344-345, doi:10.1038/307344a0, 1984.

Sugimoto, A., Yanagisawa, N., Fujita, N., Maximov, T.C.: Importance of permafrost as a source of water for plants in east Siberian taiga. Ecological Research. 17 (4), 493-503, 2002.

952 Toohey, M., Sigl, M.: Volcanic stratospheric sulphur injections and aerosol optical depth
953 from 500 BCE to 1900 CE. Earth System Science Data. doi:10.5194/essd-9-809-
954 2017, 2017.
955 Vaganov, E.A., Hughes, M.K., Kirdyanov, A.K., Schweingruber, F.H., Silkin, P.P.: Influence
956 of snowfall and melt timing on tree growth in subarctic Eurasia. Nature. 400, 149-
957 151, 1999.
958 Vaganov, E.A., Hughes, M.K., Shashkin, A.V.: Growth dynamics of conifer tree rings.
959 Springer Verlag, Berlin., pp. 353, 2006.
960 Wegmann, M., Brönnimann, S., Bhend, J., Franke, J., Folini, D., Wild, M., Luterbacher, J.:
961 Volcanic influence on European summer precipitation through monsoons: Possible
962 cause for “years without summer”. AMS, doi.org/10.1175/JCLI-D-13-00524.1, 2014.
963 Wigley, T.M.L., Briffa, K.R., Jones, P.D.: On the Average Value of Correlated Time Series,
964 with Applications in Dendroclimatology and Hydrometeorology. Journal of Climate
965 and Applied Meteorology. 23 (2), 201-213, doi:10.1175/15200450(1984)023.0201,
966 1984.
967 Wiles, G.C., D’Arrigo, R.D., Barclay, D., Wilson, R.S., Jarvis, S.K., Vargo, L., Frank, D.:
968 Surface air temperature variability reconstructed with tree rings for the Gulf of
969 Alaska over the past 1200 years. The Holocene. 6, 10.1177/0959683613516815,
970 2014.
971 Wilson, R.J.S., Anchukaitis, K., Briffa, K. et al.: Last millennium Northern Hemisphere sum-
972 mer temperatures from tree rings. Part I: the long-term context. Quaternary Science
973 Review. 134, 1–18, 2016.
974 Zielinski, G.A., Mayewski, P.A., Meeker, L.D., Whitlow, S., Twickler, M.S., Morrison, M.,
975 Meese, D.A., Gow A.J., Alley, R.B.: Record of volcanism since 7000 BC from the

976 GISP2 Greenland ice core implications for the volcano-climate system. Science. 264
977 (5161), 948-952, 1994.
978 Zielinski, G.A.: Use of paleo-records in determining variability within the volcanism-climate
979 system. Quaternary Science Reviews. 19, 417-438, 2000.